Geological Society of America
Special Paper 360
2002

Constraints on the age of formation of seismically reflective middle and lower crust beneath the Bering Shelf: SHRIMP zircon dating of xenoliths from Saint Lawrence Island

Elizabeth L. Miller and Trevor R. Ireland*
Department of Geological and Environmental Sciences, Stanford University, Stanford, California 94305-2115, USA
Simon L. Klemperer
Department of Geophysics, Stanford University, Stanford, California 94305-2115, USA
Karl R. Wirth
Geology Department, Macalester College, Saint Paul, Minnesota 55105, USA
Vyacheslav V. Akinin
Russian Academy of Science, Northeast Interdisciplinary Science Research Institute, Portovaya Street, 16, Magadan, 685000, Russia
Thomas M. Brocher
U.S. Geological Survey, 345 Middlefield Road, Menlo Park, California 94025, USA

ABSTRACT

Seismic reflection and/or refraction studies reveal reflective middle and lower crust and a sharp Moho (~32 km depth) beneath a broad region of the Bering Shelf between Alaska and northeast Russia. Basalt flows on Saint Lawrence Island of the late Cenozoic Bering Sea basalt province contain upper mantle and crustal xenoliths that include mafic cumulate rocks and lesser pyroxene-bearing gneisses that equilibrated at ~4–6 kbar. The gneissic xenoliths are interpreted as intrusive rocks that acquired deformation and/or recrystallization fabrics during granulite facies metamorphism.

Three gneissic xenoliths from two sites yielded zircons that were dated by the U-Pb method with the SHRIMP II (sensitive high resolution ion microprobe). Zoned prismatic zircons of magmatic origin yield ages mostly ca. 85–90 Ma. Rounded, nonzoned zircons from other samples are likely metamorphic in origin and yield mostly ~64 Ma ages. No older ages were obtained. More abundant gabbroic xenoliths are interpreted to represent mafic magmas emplaced into the middle to lower crust during this same approximate time span.

The oldest surface rocks on Saint Lawrence Island include Paleozoic-Mesozoic shelfal units of the Brooks Range (once deposited on Precambrian basement) but xenolith age data suggest that such older rocks, if ever volumetrically important in the deeper crust, could have been reconstituted and remobilized during younger thermal and/or magmatic events. Conversely, Late Cretaceous to Paleocene magmatic rocks are likely increasingly important with depth in the crust. A similarly young age is inferred for the development of seismically imaged reflective crust and (by inference) the Moho beneath the Bering Shelf.

*Current address: Research School of Earth Sciences, The Australian National University, 1 Mills Road, Canberra, ACT 0200, Australia.

Miller, E.L., Ireland, T.R., Klemperer, S.L., Wirth, K.R., Akinin, V.V., and Brocher, T.M., 2002, Constraints on the age of formation of seismically reflective middle and lower crust beneath the Bering Shelf: SHRIMP zircon dating of xenoliths from Saint Lawrence Island, *in* Miller, E.L., Grantz, A., and Klemperer, S.L., eds., Tectonic Evolution of the Bering Shelf–Chukchi Sea–Arctic Margin and Adjacent Landmasses: Boulder, Colorado, Geological Society of America Special Paper 360, p. 195–208.

INTRODUCTION

Deep seismic reflection profiling has brought new insight into the nature of tectonic, magmatic, and metamorphic processes occurring in the deep crust and mantle that are not easily inferred from surface geology alone. The results of such studies have had important implications for our understanding of the evolution and growth of continental crust and have also underscored the importance of magmatism and extension in modifying and stabilizing continental crust (e.g., Costa et al., 1994; Costa and Rey, 1995; Mooney and Meissner, 1992). Seismic reflection and refraction data were collected across the Bering Shelf–Chukchi Sea region as part of an international collaborative effort; the effort included two parallel seismic reflection profiles that are the first to image the deep crust and mantle beneath the region (Klemperer et al., this volume, Chapter 1; Wolf et al., this volume, Chapter 2) (Fig. 1). Mantle- and crust-derived xenoliths are common in Neogene basalt fields of the Bering Sea basalt province, and their study provides a unique opportunity to place constraints on the nature and age of the seismically imaged crust. This chapter presents U-Pb age data on zircons from pyroxene-bearing gneissic xenoliths inferred to have originated in the middle crust beneath Saint Lawrence Island on the Bering Shelf (Fig. 1). These new data provide us with information on the age and history of the crust beneath this region, underscore the importance of magmatic processes in determining this his-

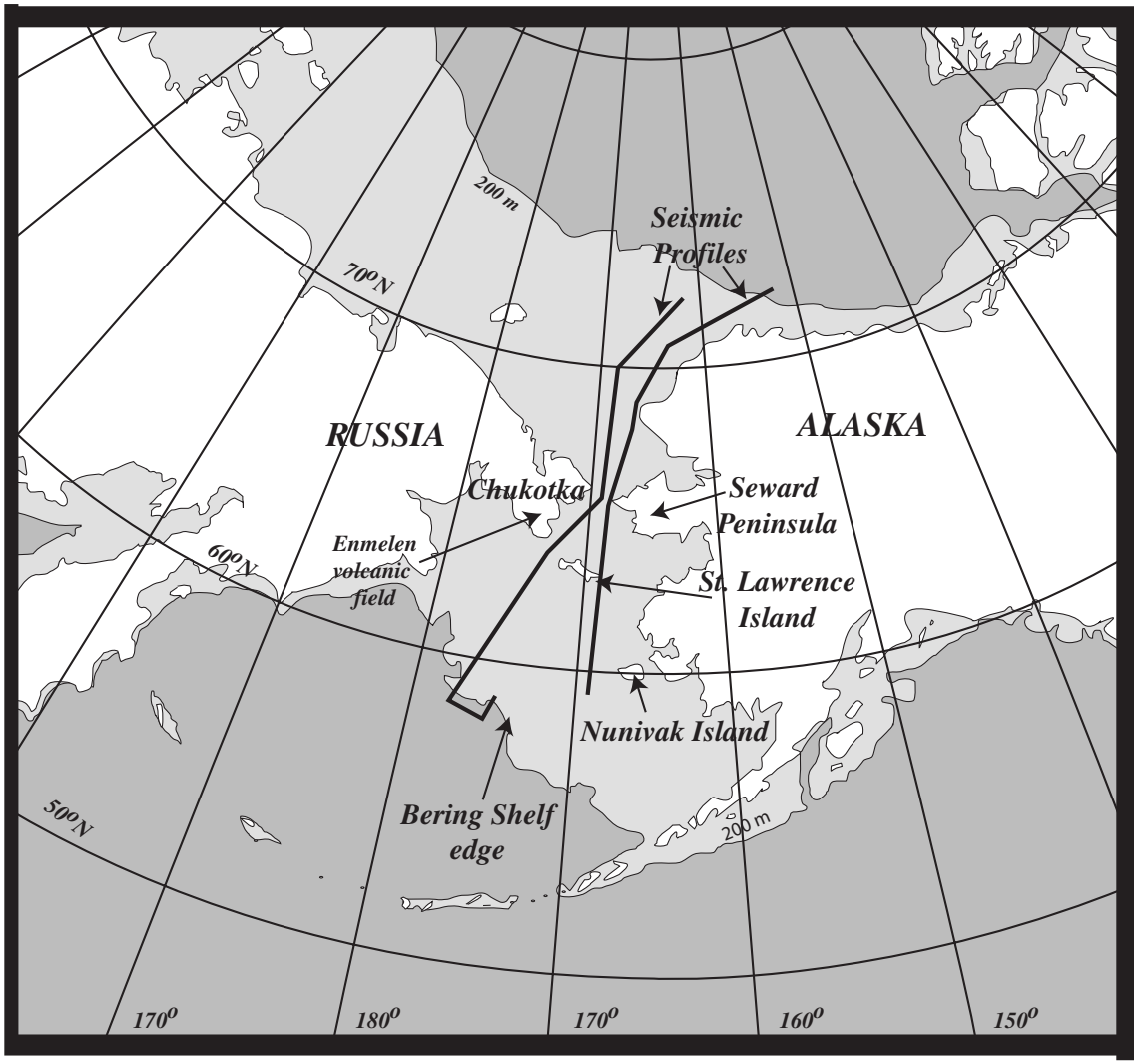

Figure 1. Location map of seismic reflection profiles of the Bering-Chukchi deep crustal transect and some of most important Neogene basalt fields of the Bering Sea basalt province: Saint Lawrence Island, Nunivak Island, the Candle and Immuruk basin volcanic fields in central Seward Peninsula of Alaska, and Emmelen volcanic field on Chukotka Peninsula, Russia. Base map is from U.S. Geological Survey and National Oceanographic and Atmospheric Administration.

tory, and emphasize the relative youthfulness of this history compared to the older accretionary evolution of the crust as recorded by its supracrustal geology.

GEOLOGIC SETTING

The Bering Shelf–Chukchi Sea region comprises over 50% of the total U.S. continental shelf and forms a broad isthmus of continental crust connecting the North American and Asian continents (Fig. 1). Overall, the geologic evolution of the Bering-Chukchi Shelf is only poorly understood, except for studies of the Tertiary basins of the Bering Shelf (e.g., Worral, 1991) and the Paleozoic and Mesozoic basins of the Chukchi Shelf (e.g., Sherwood et al., this volume, Chapter 3), which have been studied in detail.

The North American Cordillera is considered to be a prime example of crustal growth by the lateral accretion of terranes and island-arc systems, and the Alaskan portion of this belt is no exception. Alaska (and the Bering Shelf) is considered to have been shaped almost entirely by the process of terrane accretion since the Middle Jurassic (e.g., Howell et al., 1987; Nokleberg et al., 1998). This accretionary history was the fundamental process involved in creation of the Brooks Range foreland thrust belt in northern Alaska (Figs. 1 and 2) and in the assemblage of accreted oceanic and arc terranes along the southern margin of the range (e.g., Moore et al., 1994) (Fig. 2). Paleozoic and early Mesozoic autochthonous and allochthonous rock units of the Brooks Range orogen are found as far south as Saint Lawrence Island (Patton and Csejtey, 1980), but here the orogen is close to or beneath sea level, indicating that the processes of forma-

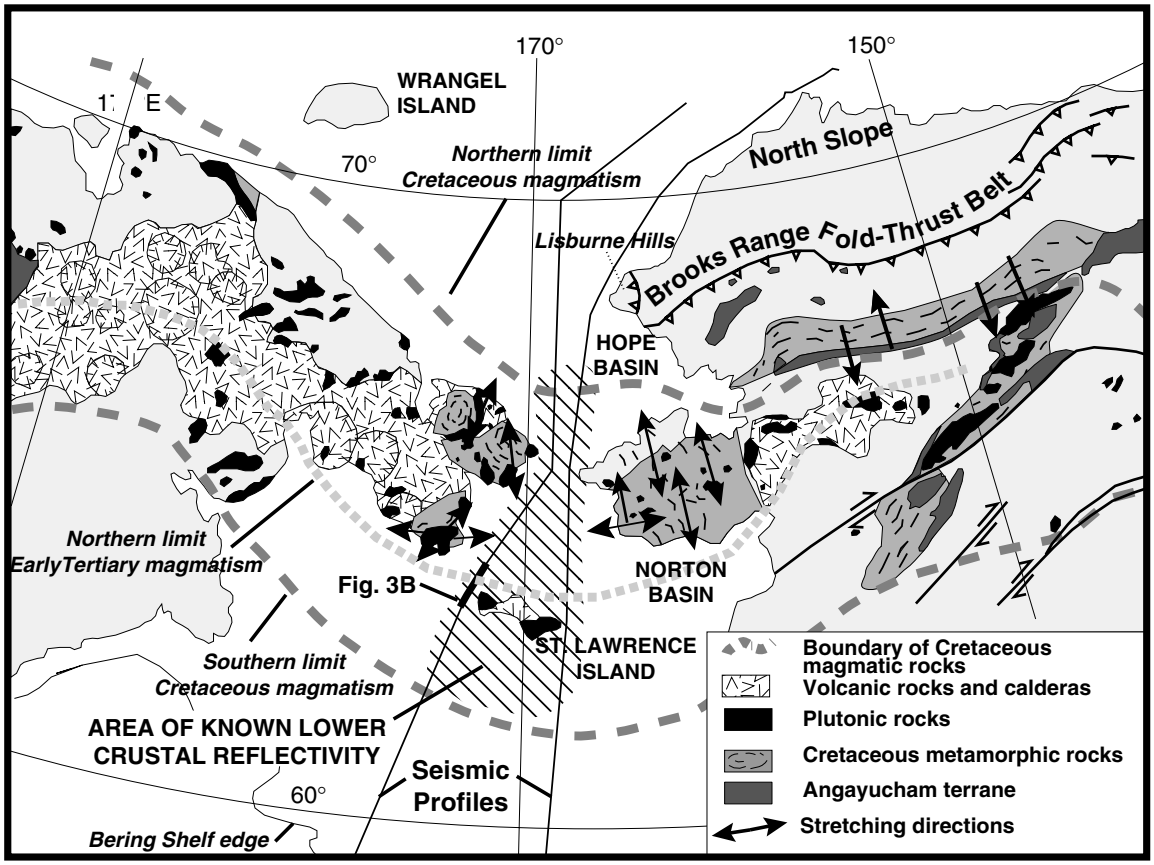

Figure 2. Location of seismic reflection lines of Bering-Chukchi deep seismic transect with respect to geologic features discussed in text. Region known to be underlain by reflective crust as imaged in seismic lines is shown by diagonal-line pattern, but probably underlies much broader region of inner Bering Shelf. Approximate northern and southern limits of mid–Late Cretaceous magmatism are shown by dark dashed lines. Approximate northern limit of very latest Cretaceous and early Tertiary magmatism is shown by light-gray dashed line. Its southern boundary is the Bering Shelf edge, based on distribution of Kuskokwim Mountains and Yukon-Kanuti magmatic belts of Alaska described by Moll-Stalcup (1994), and their inferred offshore continuation (Cooper et al., 1987; Worral, 1991). Stretching direction in metamorphic rocks within the belt of Cretaceous magmatism from Little et al. (1994), Law et al. (1994), Toro et al. (this volume), and Christiansen and Snee (1993) for Brooks Range; Till and Dumoulin (1999) and Dumitru et al. (1995) for Seward Peninsula; and Miller et al. (this volume, Chapter 17) for Russia.

tion and modification of continental crust in this region must differ from those characterizing the rest of the Brooks Range. Was terrane accretion the only mechanism of crustal growth across this portion of the orogen, and if so, why didn't this region undergo crustal thickening? Or, has subsequent crustal extension played a role here, and if so, at what time?

Cutting across the accreted terranes of Alaska and Russia are broad magmatic belts of Cretaceous age, the plutons of which span the time interval ca. 118–80 Ma (e.g., Nokleberg et al., 1997; Miller, 1994; Amato and Wright, 1997) (Fig. 2). Cretaceous plutons are commonly viewed as being of secondary importance to the mostly accretionary evolution of the Alaskan orogen (e.g., Nokleberg et al., 1998). Continuing work, however, has shown that Cretaceous magmatism was accompanied by significant regional metamorphism and deformation that may have played a fundamental role in the evolution of the deep crust beneath this region. This deformation is extreme near the Bering Strait, where it is responsible for the genesis of a series of metamorphic culminations or gneiss domes that expose sillimanite to granulite facies mid-crustal rocks (e.g., Bering Strait Geologic Field Party, 1997; Akinin and Calvert, this volume, Chapter 8; Amato et al., this volume, Chapter 7). Deformation associated with the formation of these gneiss domes is interpreted as related to the vertical rise of mid-crustal-level rocks to shallow crustal depths during regional extension. Data on the direction of crustal extension are compiled in Figure 2 and indicate north-south stretching within the Cretaceous magmatic belt at this latitude.

Miller (1994) and Amato and Wright (1997, 1998) summarized geochronologic, geochemical, and isotopic data from Cretaceous granites in Alaska, and Rowe (1998) summarized similar data from Russia. Isotopic values indicate a mantle component or origin for the magmas, modified by a variable but often significant crustal component. The variation of these values in given areas suggests a decreasing crustal component through time, at least for the Alaskan plutons (Amato and Wright, 1997). Amato and Wright (1997) suggested that plutonism is associated with northward subduction beneath the Bering Strait region and that the source region for mafic magmatism in the belt is inferred to have been enriched lithospheric mantle. The interpretation of these data from the Cretaceous plutonic belt, combined with regional geologic data, argues for significant heating (and melting and remobilization) of the crust in the Bering Strait region during the documented time span of mantle-derived magmatism (e.g., Bering Strait Geologic Field Party, 1997).

Less is known about the tectonic setting of the early Tertiary belt of volcanic and plutonic rocks that are inferred to underlie the outer part of the Bering Shelf (Fig. 2). On land, continental volcanic rocks and associated plutons form a broad belt defined by the Kuskokwim Mountains and the Yukon-Kanuti magmatic belts of Alaska, and are dated as very latest Cretaceous to early Tertiary (Paleocene) (Moll-Stalcup, 1994). The offshore continuation of this belt is inferred from magnetic anomalies along the outer edge of the Bering Shelf and by the dredging and coring of rocks of this age along the Bering Shelf edge (Marlow et al., 1976; Worral, 1991). Equivalent rocks occur in the Anadyr basin, Russia (Agapitov et al., 1973), on Saint Matthew Island (Patton et al., 1976), and in the subsurface in the Saint George and Bristol basins (Burk, 1965; McLean, 1977, 1979). These rocks were referred to as the Anadyr-Bristol volcanogenic belt by Ivanov (1985).

SEISMIC DATA

Figure 3 summarizes seismic refraction (Fig. 3A) and reflection (Fig. 3B) data (Klemperer et al., this volume, Chapter 1) representative of the crust beneath Saint Lawrence Island and the Bering Strait. The approximate range of depths from which the studied xenoliths are inferred to have been derived is shown in Figure 3B (for pressure-temperature determinations, see Wirth et al., this volume, Chapter 9).

During collection of the seismic reflection data, seismic recorders were deployed on islands and on both sides of the Bering and Chukchi Seas (Fig. 3C). The crust and upper mantle in the Bering Sea between Saint Lawrence Island, Tin City, Alaska, and northeastern Russia was sampled using several recorders in Alaska and Russia. These instruments digitally recorded signals from the 137.7 L air-gun array towed behind the ship with large source-receiver offsets (Brocher et al., 1995). The ray coverage obtained by recording seismic arrivals onshore at large ranges (wide angles) from the seismic lines is shown schematically in Figure 3B. Seismic arrivals refracted from the upper mantle (Pn) begin to arrive before those from the upper crust (Pg arrivals) at ranges of ~140 km along our transect (Brocher et al., 1995) and are consistent with a crustal thickness of 30–35 km.

Traveltimes of first and second arrivals were forward modeled using one-dimensional velocity models (Luetgert, 1992) due to the lack of true ray path reversal along much of the transect (Fig. 3C) and the oblique geometry of the reflection lines to the receivers. Separate one-dimensional models were obtained for sources north and south of each receiver. These one-dimensional models were then organized by distance resulting in a two-dimensional velocity model (Fig. 3A). Subsequent two-dimensional modeling of the traveltime data agrees well with the model shown in Figure 3A (Wolf et al., this volume, Chapter 2). The oblique recording geometry means that there are no arrivals recorded at ranges <20–30 km, greatly limiting our knowledge of velocities in the uppermost few kilometers of the crust.

The wide-angle data indicate lower crust velocities on the order of 6.1–6.4 km/s at 16–17 km depth (Conrad discontinuity) increasing to 6.7–6.9 km/s at ~32 km depth (Moho) (Fig. 3). There is a fairly clear demarcation of velocities, with velocities ≤6 km/s above the Conrad and ≥7.9 km/s below the Moho.

Seismic reflection data that imaged the deep crust and mantle (Klemperer et al., this volume, Chapter 1) indicate several unique aspects of the crust beneath Saint Lawrence Island that must be considered when interpreting the significance of the U-Pb ages we have obtained from crustal xenoliths. The seismic

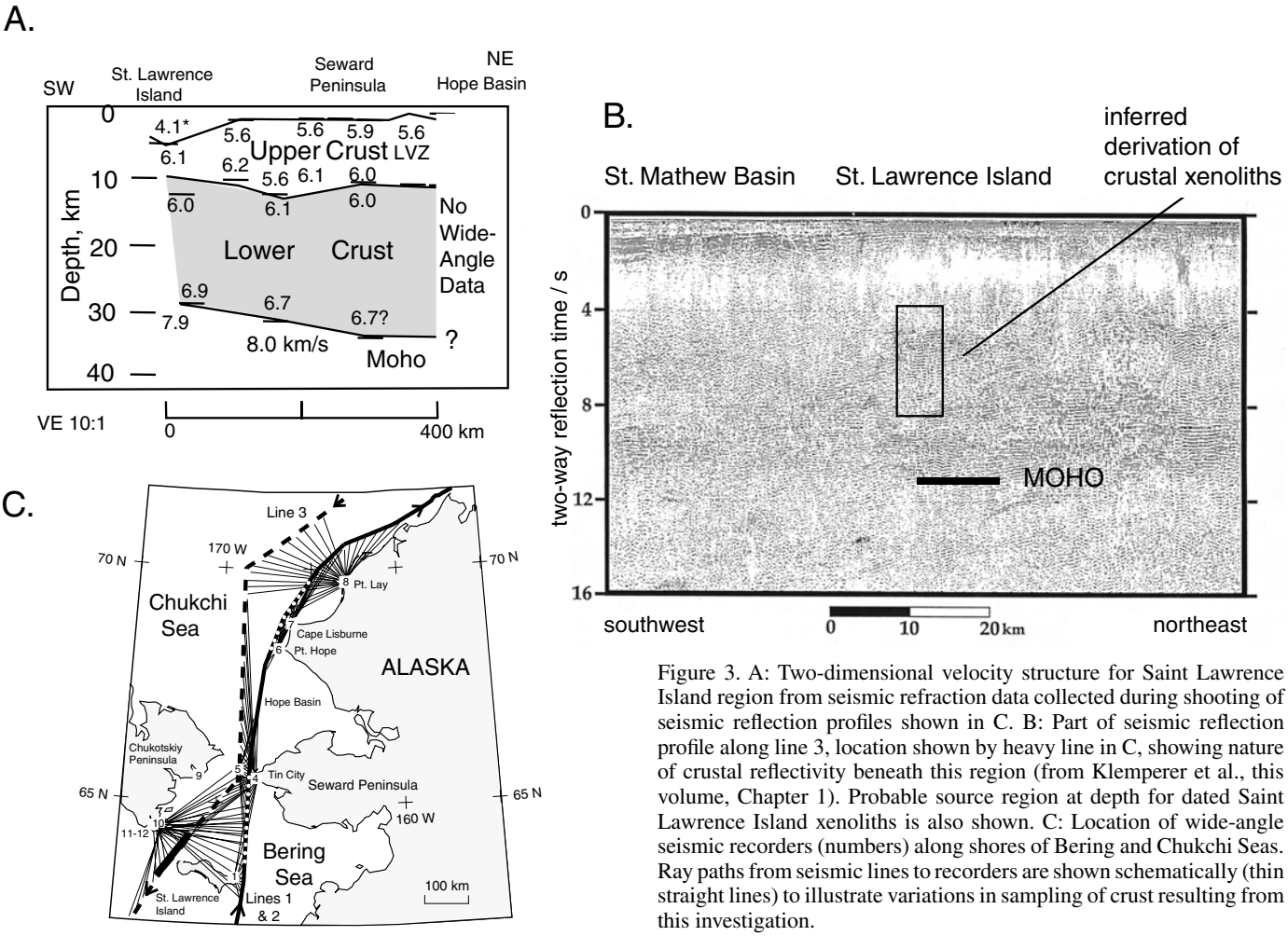

Figure 3. A: Two-dimensional velocity structure for Saint Lawrence Island region from seismic refraction data collected during shooting of seismic reflection profiles shown in C. B: Part of seismic reflection profile along line 3, location shown by heavy line in C, showing nature of crustal reflectivity beneath this region (from Klemperer et al., this volume, Chapter 1). Probable source region at depth for dated Saint Lawrence Island xenoliths is also shown. C: Location of wide-angle seismic recorders (numbers) along shores of Bering and Chukchi Seas. Ray paths from seismic lines to recorders are shown schematically (thin straight lines) to illustrate variations in sampling of crust resulting from this investigation.

reflection data (Klemperer et al., this volume, Chapter 1) indicate a gradual but significant change in the character of lower-crustal reflections and the reflection Moho just south of the Hope Basin (Fig. 3A). South from there, the reflection Moho is normally picked as the base of a sequence of many reflections that occupy the lower one- to two-thirds of the crust, marking the transition to a usually nonreflective upper mantle (Fig. 3B). The layered character of the crust is most prominent from the Bering Strait to Saint Lawrence Island and southward (Fig. 3B), a distance of ~500 km, and disappears near Saint Matthew Basin. Across this same distance, the crust is also a uniform thickness, estimated as 32 km (Klemperer et al., this volume, Chapter 1). It is noteworthy that the shallowest reflections of this nature are observed and occur within the uppermost 5–10 km of crust just north of Saint Lawrence Island (Fig. 3B) (and near the Seward Peninsula) (Klemperer et al., this volume, Chapter 1). In general, however, as with many if not most crustal-scale reflection profiles, the uppermost crystalline crust contains few reflections, in large part due to technical reasons involved in the data collection (Klemperer et al., this volume, Chapter 1). It is not surprising, therefore, that the data do not image specific plutons, metamorphic complexes, or gneiss domes along our line of transect.

Examples of similarly reflective crust were first observed to be widespread in the thin crust of young extensional provinces such as the North Sea and the Basin and Range Province of the western United States (e.g., Matthews and Cheadle, 1986; Allmendinger et al., 1987). In general, this type of reflectivity is thought to represent tectonically imposed layering formed by subhorizontal flow and vertical shortening during crustal thinning or extension, and/or primary igneous layering produced by mafic intrusions into the lower crust (e.g. Green et al., 1990; Warner, 1990). Crustal collapse or crustal thinning following an episode of tectonic thickening is the most likely sequence of events leading to the formation of such highly reflective crust (Warner, 1990; Nelson, 1992; Rey, 1993). In the Bering Strait–Saint Lawrence region, we attribute the reflectivity to the postulated collapse and extension of crust previously thickened during Brookian shortening in the Late Jurassic to Early Cretaceous. Collapse and extension of the crust took place during plutonism associated with the middle to Late Cretaceous magmatic

belt, when mafic underplating of the crust is also likely to have occurred (Miller and Hudson, 1991; Rubin et al., 1995; Bering Strait Field Geology Party, 1997; Amato and Wright, 1997, 1998). The region of uniform crustal thickness and high reflectivity coincides with the locus of Cretaceous magmatism at the Earth's surface (Fig. 2). The lower part of the crust beneath Saint Lawrence Island has velocities that range from 6.1 to 6.7 km/s (Fig. 3B). These velocities are consistent with some interplating of mafic sills into lower crust, leading to a bimodal velocity structure at a small scale generated by ~6.5 km/s felsic to intermediate igneous and metamorphic lithologies and ~7 km/s gabbroic intrusions (Klemperer et al., this volume, Chapter 1), but are not consistent with large volumes of gabbroic intrusives, which would have velocities of ~7 km/s. Mafic sills are a likely source for the gabbroic xenoliths with cumulate textures collected from the Neogene basalt flows on Saint Lawrence Island (Wirth et al., this volume, Chapter 9). The middle part of the crust (16–24 km depth) is characterized by fairly low velocities of 6.1–6.4 km/s (Wolf et al., this volume, Chapter 2), precluding a large component of new mafic intrusions at these depths. Thus, the reflectivity observed higher in the crust must represent ductile extensional fabrics and transposed compositional layering in metamorphic (metasedimentary and metaigneous) rocks. Examples of these rocks are present in the large gneiss domes or metamorphic culminations of the Chukotka and Seward Peninsulas (Akinin and Calvert, this volume, Chapter 8; Amato et al., this volume, Chapter 7; Bering Strait Field Geology Party, 1997).

PETROLOGY OF LAVAS AND XENOLITHS FROM SAINT LAWRENCE ISLAND

The late Cenozoic Bering Sea basalt province (Moll-Stalcup, 1994; Akinin and Apt, 1994, 1997; Akinin et al., 1997) consists of more than 17 volcanic fields on islands in the Bering Sea, on the west coast of Alaska, and on the northeastern coast of Russia. Several of these are shown in Figure 1. These volcanic fields represent the most significant volume of magma erupted in the Arctic region within the past 10 m.y. and consist primarily of tholeiitic and alkali-olivine basalt flows with subordinate basanite and nephelinite cones, flows, and maars. Alkali basalts and nephelinite from the province contain upper mantle and lower and/or upper crustal xenoliths, generally a common occurrence in alkali basalt provinces worldwide. Most of the volcanic fields are dominated by intraplate basalts that compositionally resemble those erupted in oceanic islands and in some continental settings (e.g., Wood, 1980; Clague and Frey, 1982). Pb, Sr, and Nd isotopic differences between individual volcanic fields in the Bering Sea basalt province are greater than the difference within volcanic fields, which suggests different mantle sources for the lavas (Davis et al., 1995; Akinin and Apt, 1997).

The volcanic field on Saint Lawrence Island consists of a large Paleocene to Quaternary shield volcano of alkali-olivine and tholeiitic basalt flows and more than 70 small younger cones and short flows of mostly basanite and nephelinite (Moll-Stalcup, 1994). The xenolith population in these lavas consists of spinel lherzolite, harzburgite, wehrlite, pyroxenite, amphibole-bearing pyroxenite, gabbro-norite, anorthosite, and crustal rocks including granites, gneisses, felsic volcanic, and sedimentary rock (Wirth et al., 1995). Ultramafic xenoliths are typically foliated and contain mineral grains that exhibit deformation interpreted to be due to flow in the mantle. Many of the plagioclase-bearing xenoliths have cumulate textures and are variably deformed, suggesting they originated in magma chambers in the lower crust (Wirth et al., 1995).

Many of the plagioclase- and pyroxene-bearing xenoliths are coarse-grained gabbro and gabbronorite with cumulate and poikolitic textures suggesting a magmatic origin. Deformation in these xenoliths is largely limited to undulatory extinction and slight bending of twin lamellae in plagioclase. In contrast, many of the medium-grained and feldspar-rich xenoliths exhibit a more pronounced metamorphic layering and foliation (Fig. 4). In thin section, these xenoliths exhibit a range of textures from polygonal granoblastic equigranular to interlobate and seriate; some relict igneous textures are also present. The primary pyroxene present in all of these xenoliths is hypersthene; minor diopside is also present in some xenoliths. Feldspars typically exhibit variable undulatory extinction and twin lamellae that are sometimes bent or broken. Plagioclase feldspars are typically andesine in composition, whereas alkali feldspars are sodium rich (anorthoclase composition) and exhibit coarse exsolution lamellae (mesoperthite). Minor quartz (1%–10%), Fe-Ti oxides, and apatite are also typically present. Hydrous minerals are absent, except as rare alteration products around the margins of pyroxene.

The compositions and textures of the plagioclase-pyroxene–bearing xenoliths are interpreted to indicate that they are largely of igneous origin. This interpretation is consistent with the lack of convincing evidence that any of the observed xenoliths are metasedimentary. The aluminum compositions of the clinopyroxenes plot in the field of granulites (Al [IV] versus Al [VI]; Aoki and Kushiro, 1968). Furthermore, the Al contents of clinopyroxene and orthopyroxene pairs (Gasparik, 1984) suggest equilibration pressures of 4–6 kbar. Therefore, although we cannot unambiguously demonstrate that these xenoliths are granulite facies metamorphic rocks, we believe that the observed textures and compositions are consistent with an origin in which mafic to intermediate magmas were intruded into the mid-crust and were subsequently deformed and recrystallized at relatively high temperatures and pressures.

Xenoliths provide us with the only means of directly sampling the lower crust and mantle. Although detailed studies of xenoliths are numerous, relatively few studies have determined the ages of xenoliths that sample lower crust and mantle (e.g., Rudnick and Williams, 1987; Rudnick and Fountain, 1995; Costa and Rey, 1995; O'Reilly et al., 1995; Davis, 1996). Our initial work suggests that there are plentiful zircon populations in the probable granulite facies gneissic xenoliths brought to the surface by young basalts of the Bering Sea basalt province. The descriptions and data discussed in the following are preliminary

Figure 4. Pyroxene-bearing gneissic xenoliths collected from basalt flows on Saint Lawrence Island by Karl Wirth in 1994, illustrating nature of conspicuous gneissic foliation observed at hand-specimen scale.

and few in number compared to the information potentially available from other such rocks across this vast region.

SHRIMP DATING OF ZIRCONS

Four pyroxene-bearing gneissic xenoliths from Saint Lawrence Island were processed for zircon. Three of these yielded zircons that were dated. Sample SV19B has a visible foliation in hand specimen. In thin section it is fine grained (~0.5 mm) and granoblastic, with foliation defined by layers or concentrations of pyroxene versus plagioclase. It is composed of hypersthene (20%–30%), andesine (70%–80%) with some granophyric overgrowths on feldspars, minor quartz, and ilmenite-magnetite. Brown glass is associated with, and rims, some pyroxenes. Sample 21C is medium to coarse grained (2–4 mm) and granoblastic. Foliation or layering is present in hand specimen, but not visible in thin section due to the coarse-grained nature of the rock (Fig. 5). It is composed of diopside (trace), hypersthene (20%–30%), andesine (70%–80%), minor perthite, and oxides (2%–5%). Plagioclase grains are often strained and bent and sometimes broken. Sample SV21E is similar to SV21C and is a coarse-grained (2–4 mm), granoblastic, pyroxene-bearing gneiss. Although foliation or layering is present in hand specimen, it is not obvious in thin section due to the coarse-grained nature of the sample. It is composed of mesoperthite (70%–80%), andesine (5%–10%), diopside (10%–15%), hypersthene (2%–5%), and quartz (5%–10%). Feldspars are often strained and bent.

Zircons were mounted in epoxy and polished to reveal mid-sections. Prior to ion microprobe analysis, the zircons were photographed in transmitted light (e.g., Fig. 6) and imaged by cathodoluminescence for internal structures largely related to trace element zoning (e.g., Fig. 7). U-Pb analyses were carried out on the SHRIMP II at the Australian National University (Table 1). Owing to the youthfulness of the zircons, most effort was placed on obtaining a precise U-Pb age; $^{207}Pb/^{206}Pb$ ages are imprecise owing to the small amount of radiogenic ^{207}Pb present and the uncertainties propagated from the $^{204}Pb/^{206}Pb$ correction. As such, the fraction of common Pb in an analysis was estimated by assessing the measured $^{207}Pb/^{206}Pb$ ratio in relation to the projected position, from the common Pb isotopic composition, on to the Tera-Wasserburg concordia, which also thus yields the $^{206}Pb/^{238}U$ age (e.g., see Muir et al., 1996a,b). The common Pb composition used was a model Pb composition based on the inferred radiogenic $^{206}Pb/^{238}U$ age for each analysis. A general feature of analyses of the granulite zircons is instability in the ^{206}Pb count rate, not correlated with U concentration. The uncertainty in the $^{206}Pb/^{238}U$ ratio is often dominated by variation in the ratio, rather than statistical variations related to counting errors. Although a unique interpretation cannot be given for any given analysis, it appears that the variability is related to fine-scale Pb loss, particularly in SV19B. Data are presented in Figure 8 in the form of probability density functions by assigning unit area Gaussian curves to each $^{206}Pb/^{238}U$ age datum and then summing all data through the range in 1 Ma bins. The operation of summing the individual Gaussian curves should result in a Gaussian curve if the data are distributed about the mean in a manner consistent with the individual uncertainties. All of the data from the xenoliths show large scatter. This preliminary data set is somewhat imprecise because it does not constitute a statistically cohesive data set.

Sample SV19B contains a fairly homogeneous zircon pop-

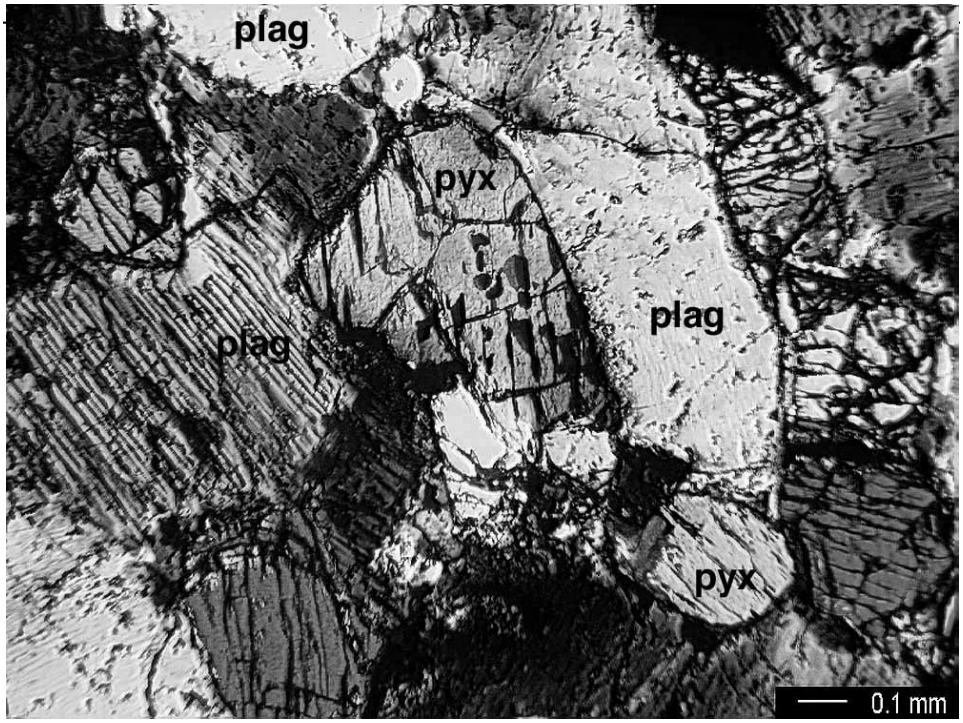

Figure 5. Thin-section photograph of sample SV21C (plag is plagioclase, pyx is pyroxene). Note coarse equigranular textures, despite strong foliation in hand specimen, indicating slow cooling or elevated temperatures long after deformation had ceased, compatible with a mid-crustal origin for xenoliths inferred from metamorphic assemblages.

ulation consisting of elongate subhedral to euhedral zircons that generally have inclusion-crowded, uranium-rich cores and clear, inclusion-free, uranium-poor rims (Figs. 6 and 7). The zircon rims typically show oscillatory zoning (Fig. 7). We infer from these characteristics that the zircons are most likely igneous in origin and, given the metamorphic fabric of the rock, that the plutonic protolith was subsequently metamorphosed and deformed at probable granulite facies conditions. We found that zircon cores from sample SV19B are systematically, but only marginally, older than the rims (Table 1), suggesting a slightly earlier magmatic precursor for this rock. The main age represented in the peak of the distribution suggests a magmatic age of ca. 85 Ma, although two of the analyses are distinctly younger (ca. 74 Ma) and suggest that Pb loss may have occurred. The suggestion that Pb loss may explain the younger ages is based on the reasoning that superimposed granulite facies metamor-

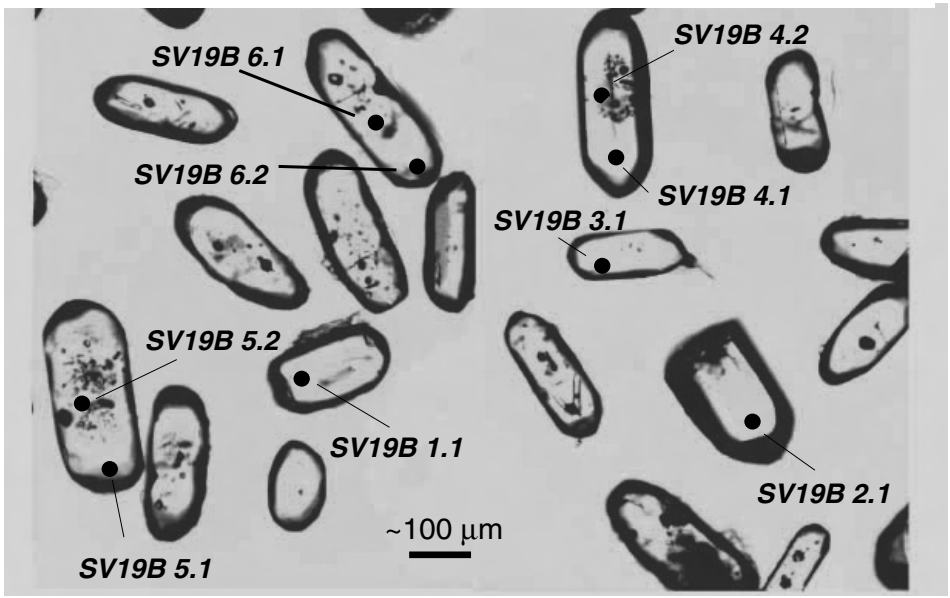

Figure 6. Transmitted light photo of zircons from sample SV19B showing spot localities dated with SHRIMP II.

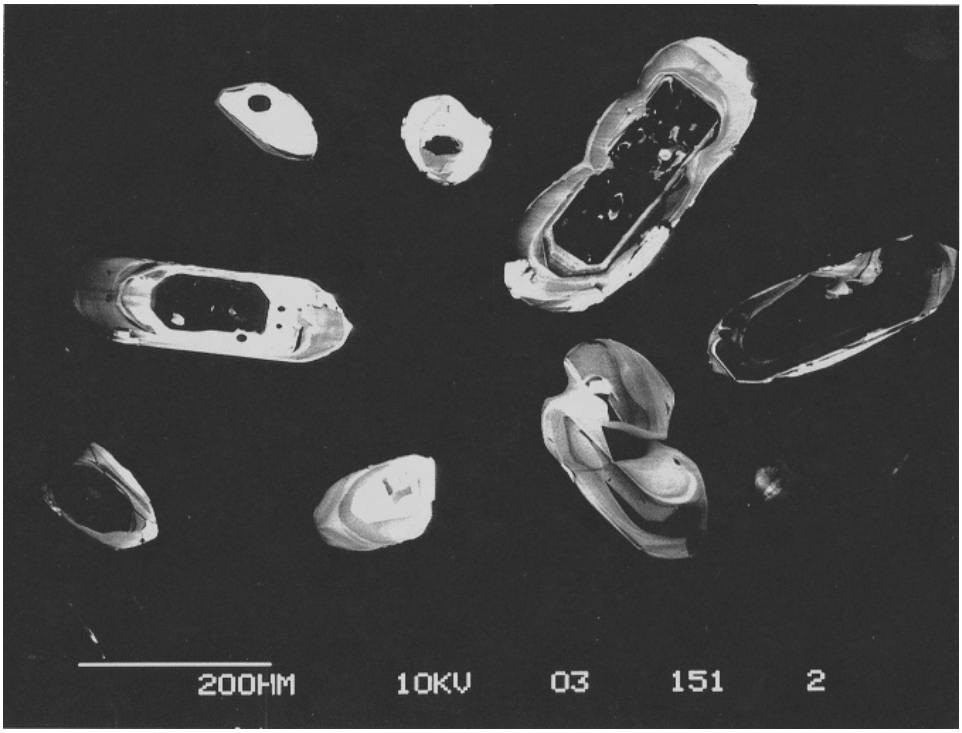

Figure 7. Cathodoluminescence scan of typical zircons from sample SV19B showing oscillatory zoning. Note that publication-quality cathodoluminescent scans shown here and in Figure 10 imaged a different part of the zircon population than those dated.

TABLE 1. U-PB ISOTOPIC DATA, SAINT LAWRENCE ISLAND XENOLITHS

Labels	U	Th	Th/U	$^{207}Pb/^{206}Pb$	$^{238}U/^{206}Pb$	Age (Ma)
SV19B						
1.1	419	121	0.29	0.0456 ± 0.0035	75.95 ± 5.66	84.5 ± 6.3
2.1	460	253	0.55	0.0502 ± 0.0029	71.19 ± 2.36	89.7 ± 3.0
3.1	390	102	0.26	0.0496 ± 0.0035	86.13 ± 5.05	74.2 ± 4.3
4.1c	422	112	0.26	0.0491 ± 0.0025	70.70 ± 6.40	90.4 ± 8.1
4.2r	2335	139	0.06	0.0499 ± 0.0015	73.69 ± 1.32	86.7 ± 1.5
5.1r	393	170	0.43	0.0501 ± 0.0024	87.65 ± 3.04	72.9 ± 2.5
5.2c	4050	760	0.19	0.0471 ± 0.0012	60.57 ± 1.71	105.7 ± 3.0
6.1r	2685	571	0.21	0.0479 ± 0.0009	76.68 ± 0.82	83.5 ± 0.9
6.2c	373	143	0.38	0.0513 ± 0.0022	70.48 ± 3.67	90.5 ± 4.7
SV21C						
1.1	31	20	0.64	0.0985 ± 0.0071	91.31 ± 3.62	66.3 ± 2.7
2.1	44	32	0.72	0.0489 ± 0.0048	113.77 ± 6.56	56.3 ± 3.2
3.1	548	202	0.37	0.0488 ± 0.0011	90.82 ± 2.07	70.5 ± 1.6
4.1	206	68	0.33	0.0487 ± 0.0025	93.88 ± 3.52	68.2 ± 2.5
6.1	357	229	0.64	0.0468 ± 0.0026	103.34 ± 2.51	62.1 ± 1.5
7.1	297	205	0.69	0.0536 ± 0.0031	99.39 ± 1.59	64.1 ± 1.0
8.1	28	21	0.75	0.0362 ± 0.0057	99.49 ± 4.21	65.3 ± 2.8
SV21E						
1.1	479	277	0.58	0.0481 ± 0.0013	70.12 ± 2.84	91.3 ± 3.7
1.2	28	6	0.21	0.0315 ± 0.0042	94.20 ± 3.07	69.2 ± 2.3
2.1	607	453	0.75	0.0465 ± 0.0011	64.06 ± 0.73	100.0 ± 1.1
3.1	9	3	0.25	0.0756 ± 0.0104	94.96 ± 2.44	63.7 ± 1.8

Note: All errors are 1σ, unless otherwise stated.
Standard error of 11 AS3 analyses = 0.33% (with 1.0% error analysis, mean square of weighted deviates = 1.15).
c, r designates analyses of cores and rims, respectively.

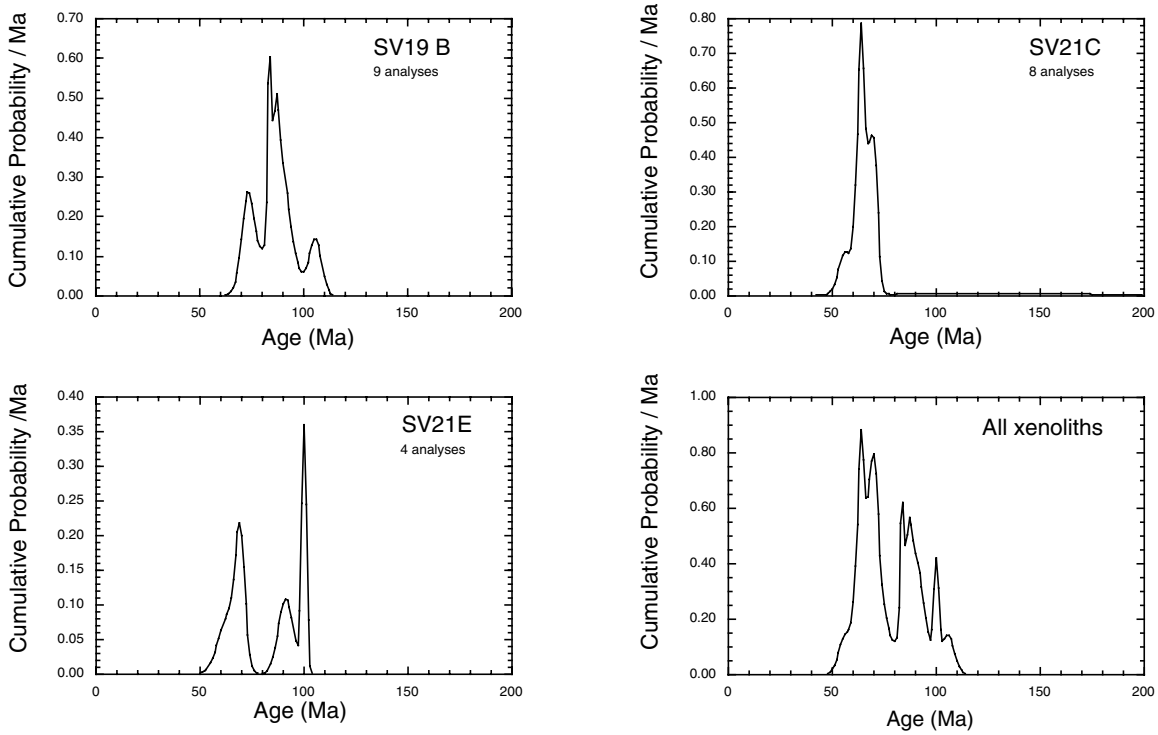

Figure 8. Cumulative probability plots of U-Pb zircon ages from samples dated.

phism did not appear to have precipitated any new zircon in this rock; the delicate oscillatory zoning observed in the zircon rims is more consistent with magmatic crystallization. Thus the ca. 74 Ma ages are likely the result of Pb loss, at this or at a younger time of heating and metamorphism. The proposed protolith age of 85 Ma may underestimate the age of magmatic crystallization of this rock, although it is unlikely, based on the data, that this magmatic age would be much older than ca. 90 Ma.

Samples SV21C and SV21E have similar zircon populations, distinct from those of sample SV19B (Figs. 9 and 10). The majority of zircons from these two samples are rounded and equidimensional to stubby in shape and are smaller than those from sample SV19B. They have poorly defined crystal faces, are adamantine in luster, and mostly very clear (Fig. 9). Few of the zircons are elongate or prismatic, but these grains, in contrast to those of sample SV19B, have poorly developed crystal faces and some grains have small rounded overgrowths. Cathodoluminescence images of zircons from sample SV21C (Fig. 10) indicate that the smaller rounded zircons are not zoned in any systematic fashion, and vary in luminescence from grain to grain and commonly across the grain (Fig. 10). The larger grains commonly show relict oscillatory zoning, and some have oscillatory-zoned cores surrounded by clear, uranium-poor rims. We interpret these characteristics as indicating that most of the zircon grew in a metamorphic environment, but that the protolith of the rock was likely plutonic. The seven analyses of zircons from sample SV21C are fairly consistent and indicate an age of ca. 64 Ma, which is significantly younger than the age of zircons in sample SV19B, 85–90 Ma. One of the analyses from a small rounded grain (SV21C 3.1), with no apparent core, gives an age of ca. 70 Ma, detectably older than the mean in sample SV21C. Grain 7, which is a long prismatic grain of inferred magmatic origin (Fig. 9) yields an age (64 Ma) no different from the rounded, inferred metamorphic zircons. Although the age of inferred magmatic grain 7 may have been reset during granulite facies metamorphism at 64 Ma, the slightly older age of grain 3 may suggest a slightly earlier metamorphic event ca. 70–75 Ma. In this respect, the ages of the younger grains of SV19B are consistent with such an age, but more data are required to assess the presence of a distinct population of 70–75 Ma metamorphic zircons.

Ages of the four zircon analyses from sample SV21E are mixed; two younger ages are similar to the metamorphic ages obtained from SV21C and two older ages of 100 and 91 Ma are similar to the magmatic populations of SV19B. The two younger samples are likely metamorphic in origin, whereas the older grains may be relict magmatic zircons of middle to Late Cretaceous age. The metamorphic zircons in SV21E are noteworthy for their low U concentrations, which are characteristic of metamorphic zircons that have grown under granulite facies conditions (Gibson and Ireland, 1995). However, these zircons do not show the extreme fractionation in Th/U (often <0.01) found in some granulite zircons.

In summary, zircons from the pyroxene-bearing crustal xenoliths indicate that magmatic protolith rocks of 85–100 Ma

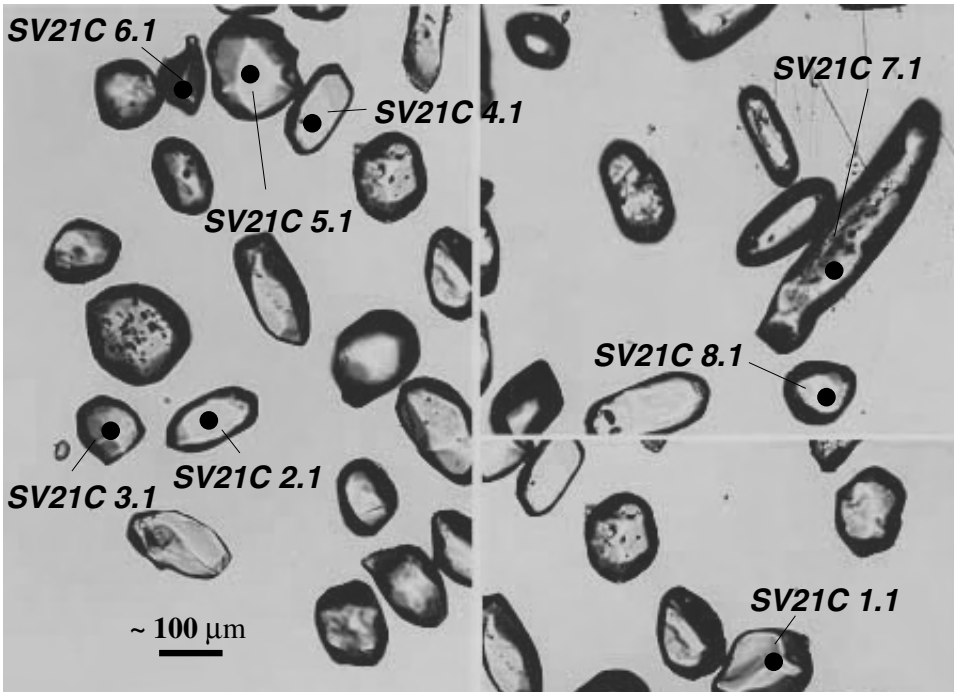

Figure 9. Transmitted light photo of zircons from samples SV21C and SV21E showing spot localities dated with SHRIMP II.

were involved in a younger thermal event between 60 and 75 Ma; a peak event ca. 64 Ma affected the deeper crust beneath the inner Bering Shelf. This younger thermal event coincided with the emplacement of the Yukon-Kanuti and Kuskokwim Mountains magmatic belts between 76 and 55 Ma (Moll-Stalcup, 1994). The northernmost exposures of volcanic rocks associated with the Yukon-Kanuti and Kuskokwim magmatic belts occur on Saint Lawrence Island, where volcanic rocks have been dated by the K-Ar method on sanidine (64.4 Ma), hornblende (62.2 Ma), and whole rock (64 Ma) (Wilson et al., 1994); these ages

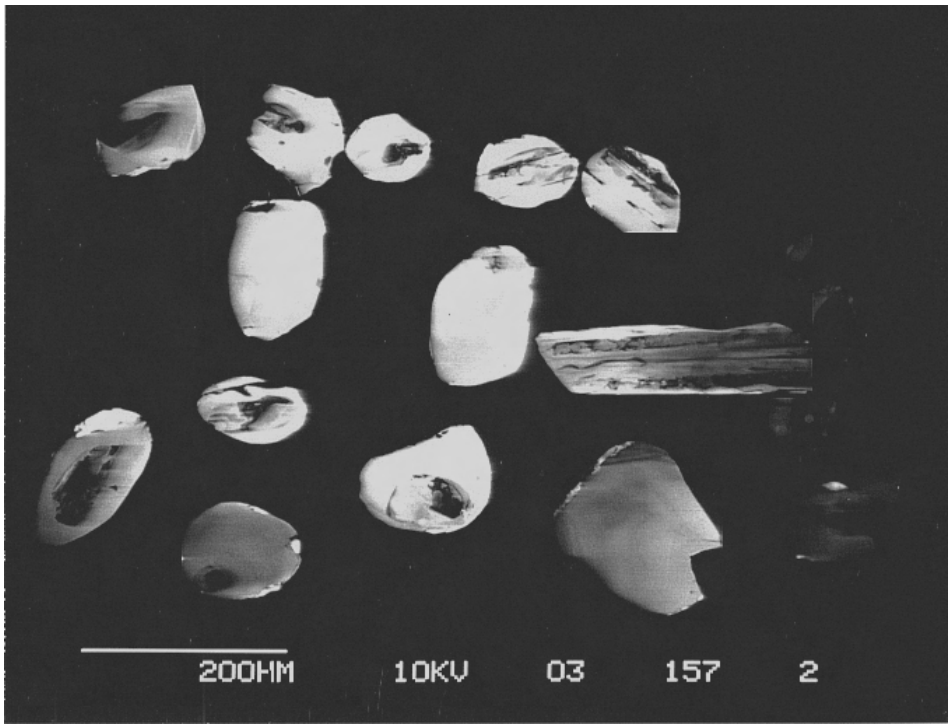

Figure 10. Cathodoluminescence scan of typical zircons from sample SV21C.

are indistinguishable from the age of the mid-crustal metamorphic zircons we dated. The ages of the older, magmatic zircons coincide with ages obtained from the broad belt of Cretaceous granitoid plutons that crosses the Bering Strait from Alaska to Russia and extends from the Seward Peninsula to Saint Lawrence Island (Fig. 2).

CONCLUSIONS

The crustal and mantle xenoliths in Neogene basalt flows on Saint Lawrence Island provide an unusual opportunity to study the nature and history of the crust and underlying mantle beneath the inner Bering Shelf. These xenoliths also provide insight for the interpretation of the deep crustal seismic reflection data collected across this region (Klemperer et al., this volume, Chapter 1).

On the basis of refraction studies, the crust beneath Saint Lawrence Island exhibits normal velocities and a sharply defined Moho between 30 and 35 km, which is fairly typical of continental crust worldwide. Seismic reflection data indicate that the middle and lower crust is characterized by well-developed subhorizontal reflectivity down to the Moho, where the underlying mantle is transparent. Worldwide, this type of reflectivity has been interpreted as a product of modification of continental crust by extensional processes (e.g., Mooney and Meissner, 1992).

This fairly persistent crustal reflectivity has been mapped seismically over a broad part of the inner Bering Shelf and southern Hope Basin and coincides in a general way with the locus of middle to Late Cretaceous magmatism in Alaska and Russia (Fig. 2). The northernmost outcrops of Paleocene volcanic rocks are on Saint Lawrence Island and continue on land in Alaska as the Kuskokwim Mountains and Yukon-Kanuti magmatic belts of latest Cretaceous to Paleocene age (Moll-Stalcup, 1994). At the scale of the Bering Shelf, it appears that magmatism youngs southward and that the locus of latest Cretaceous to Paleocene magmatism in part overprints the locus of mid–Late Cretaceous magmatism (Fig. 2). Geochronologic and isotopic data from middle to Late Cretaceous magmatic rocks (Miller, 1994; Amato and Wright, 1997, 1998; Bering Strait Geologic Field Party, 1997; Rowe, 1998) suggest that magmas that intruded the crust during this event were mantle derived, and mixed, to variable extent, with crustal rocks. The mantle-derived magmatism is inferred to be at least in part related to subduction beneath the ancient Bering margin. Magmatism likely occurred in an extensional tectonic environment as the active subduction zone migrated south with time (Amato and Wright, 1997, 1998). An extensional tectonic setting for magmatism is also inferred from geologic studies on either side of the Bering Strait that outline the relationship of Cretaceous magmatism to metamorphism, melting, and wholesale flow of the middle and lower crust within the broad metamorphic culminations or gneiss domes within the magmatic belt (Fig. 2). Less is known about the tectonic setting of the younger latest Cretaceous to Paleocene magmatic belt, except that it covers an extensive region from Saint Lawrence Island south to the edge of the present Bering Shelf, and that volcanic rocks in the belt were erupted in a subaerial setting (Cooper et al., 1987; Worral, 1991).

Pyroxene-bearing gneissic xenoliths derived from the mid-crust beneath Saint Lawrence Island most likely represent highly deformed intrusive rocks that have undergone granulite facies metamorphism. These xenoliths have zoned prismatic zircons that appear to be magmatic and yield preliminary Late Cretaceous U-Pb ages, which we interpret as intrusive ages between ca. 85 and 90 Ma with one age as old as 100 Ma. Some of these xenoliths have rounded, nonzoned zircons that appear to be metamorphic, and these yield Late Cretaceous to early Tertiary metamorphic ages between 60 and 75 Ma with a peak of ages at 64 Ma. Nonfoliated gabbroic xenoliths are the more common crustal xenolith represented in basalt flows on Saint Lawrence Island. Although these have not yet been dated, we interpret them to be derived from Late Cretaceous or early Tertiary mafic sills and plutons in the middle and lower crust. Together, these preliminary data suggest that the igneous and metamorphic events responsible for development of the observed reflective crust and sharp Moho beneath Saint Lawrence and the inner Bering Shelf occurred during the Late Cretaceous and early Tertiary.

The Alaskan mainland south of the Brooks Range has long been portrayed as an orogenic collage of allochthonous terranes presumed to continue westward beneath the Bering Shelf (e.g., Nokleberg et al., 1998). Some of these terranes have been identified on Saint Lawrence Island, where Paleozoic rocks similar to shelfal sequences in the Brooks Range occur together with a Triassic sequence of chert, shale, and greenstone similar to that in the Angayucham terrane of the southern Brooks Range (Patton and Dutro, 1969; Patton and Csejtey, 1980). Although one might have expected the deep crustal seismic reflection data collected as part of this project to image the orogenic collage of allochthonous terranes presumed to underlie the Bering Shelf, the data actually provide little to no insight into this Albian and older Mesozoic accretionary history. Seismic reflection data in conjunction with the preliminary U-Pb zircon ages of deep crustal xenoliths indicate that the most important events that formed the present-day middle and lower crust postdate the accretionary history of the region and are linked to the Cretaceous to early Tertiary magmatic history of the region.

ACKNOWLEDGMENTS

The Continental Dynamics Program, National Science Foundation (NSF), award EAR-93-17087 funded most of the research presented here. In addition, an NSF Research Opportunity Award tied to EAR-93-17087 funded filed work by K. Wirth and students who collected the xenoliths on Saint Lawrence Island (see Chapter 9 of this volume). The Office of Polar Programs, NSF, grant OPP-99-05790 supported data compilation and interpretation. V. Akinin acknowledges support by RFBR grant 01-05-65453. We thank our reviewers Walter Mooney, Betsy

Moll-Stalcup, James Mortensen, and an anonymous reviewer for improvements on our original manuscript.

REFERENCES CITED

Agapitov, D.I., Ivanov, V.V., and Krainov, V.G., 1973, New data on geology and perspective of oil and gas resources in Anadyr basin, *in* The problems of oil and gas potential in the North-East of USSR (Novye dannye po geologii i perspektivam neftegasonosnosti Anadyrskogo basseina. V kn: Problemy neftegazonosnosti Cevero-Vostoka SSSR): Magadan, Russia, Northeast Interdisciplinary Science Research Institute, v. 49, p. 23–39 (in Russian).

Akinin, V.V., 1995, Petrology of alkali lavas and deep-seated inclusions of Enmelen volcanoes, Chukchi Peninsula, *in* Simakov, K.V., and Thurston, D.K., Proceedings of the1994 International Conference on Arctic Margins: Magadan, Russia, North East Science Center, Far Eastern Branch of the Russian Academy of Science, p. 138–146.

Akinin, V.V., and Apt, J.E., 1994, Enmelen volcanoes, Chukchi Peninsula: Petrology of alkaline lavas and deep seated inclusions: Magadan, Russia, Northeast Interdisciplinary Science Research Institute, Far Eastern Branch of the Russian Academy of Science, 97 p. (in Russian).

Akinin, V.V., and Apt, Y.E., 1997, Late Cenozoic alkaline basaltic volcanism of the North East of Russia, *in* Byalobzhesky, S.G., ed., Magmatism and ores of north east of Russia: Magadan, Russia, Northeast Interdisciplinary Science Research Institute, Far Eastern Branch of the Russian Academy of Science, p. 153–172.

Akinin, V.V., Roden, M.F., Francis, D.M., Apt, J.E., and Moll-Stalcup, E., 1997, Compositional and thermal state of the upper mantle beneath the Bering Sea basalt province: Evidence from the Chukchi Peninsula of Russia: Canadian Journal of Earth Sciences, v. 34, p. 789–800.

Allmendinger, R.W., Hauge, T.A., Hauser, E.C., Potter, C.J., Klemperer, S.L., Nelson, K.D., Knuepfer, P.L.K., and Oliver, J. 1987, Overview of the COCORP 40° transect, western United States, the fabric of an orogenic belt: Geological Society of America Bulletin, v. 98, p. 308–319.

Amato, J.M., and Wright, J.E., 1997, Potassic mafic magmatism in the Kigluaik gneiss dome, Northern Alaska: A geochemical study of arc magmatism in an extensional tectonic setting: Journal of Geophysical Research, v. 102, p. 8065–8084.

Amato, J.M., and Wright, J.E., 1998, Geochronologic investigations of magmatism and metamorphism within the Kigluaik Mountains gneiss dome, Seward Peninsula, Alaska, *in* Clough, J.G., and Larson, F., eds., Short notes on Alaska geology: State of Alaska, Department of National Resources, Division of Geological and Geophysical Surveys Professional Report 118, p. 1–21.

Amato, J.M., Wright, J.E, Gans, P.B., and Miller, E.L., 1994, Magmatically induced metamorphism and deformation in the Kigluaik gneiss dome, Seward Peninsula, Alaska: Tectonics, v. 13, p. 515–527.

Aoki, K., and Kushiro, I., 1968, Some clinopyroxenes from ultramafic inclusions in Dreiser Weiher, Eifel: Contributions to Mineralogy and Petrology (former title: Beitraege zur Mineralogie und Petrologie), v. 18, no. 4, p. 326–337.

Bering Strait Geologic Field Party, 1997, Koolen metamorphic complex, NE Russia: Implications for the tectonic evolution of the Bering Strait region: Tectonics, v. 16, p. 713–729.

Brocher, T.M., Allen, R.M., Stone, D.B., Wolf, L.W., and Galloway, B.K., 1995, Data report for onshore-offshore wide-angle seismic recordings in the Bering-Chukchi Sea, western Alaska and eastern Siberia: U.S. Geological Survey Open-File Report 95–650, 57 p.

Burk, C.A., 1965, The geology of the Alaska peninsula–island arc and continental margin: Boulder, Colorado, Geological Society of America Memoir 99, 250 p.

Choukroune, P., and the ECORS Pyrenees Team, 1989, The ECORS Pyrenean deep seismic profile: Reflection data and the overall structure of an orogenic belt: Tectonics, v. 8, p. 23–39.

Christiansen, P.P., and Snee, L.W., 1993, Structure, metamorphism and geochronology of the Cosmos Hills and Ruby Ridge, Brooks Range schist belt, Alaska: Tectonics, v. 14, p. 193–213.

Clague, D.A., and Frey, F.A., 1982, Petrology and trace element geochemistry of the Honolulu Volcanics, Oahu: Implications for the oceanic mantle below Hawaii: Journal of Petrology, v. 23, p. 447–504

Cooper, A.K., Marlow, M.S., and Scholl, D.W., 1987, Geologic framework of the Bering Sea Crust, *in* Scholl, D.W., Grantz, A., and Vedder, J.C., eds., Geology and resource potential of the continental margin of western North America and adjacent ocean basins: Beaufort Sea to Baja California: Houston, Texas, Circum-Pacific Council for Energy and Mineral Resources, Earth Science Series, v. 6, p. 73–102.

Costa, S., and Rey, P., 1995, Lower crustal rejuvenation and growth during post-thickening collapse: Insights from a crustal cross section through a Variscan metamorphic core complex: Geology, v. 23, p. 905–908.

Costa, S., Rey, P., Todt, W., and Goldstein, S.L, 1994, Evolution of the lower continental crust during post-thickening collapse: Mineralogical Magazine, v. 58A, no. A-K, p. 197–198.

Davis, A.S., Marlow, M.S., and Wong, F.L., 1995, Petrology of Quaternary basalt from the Bering Sea continental margin, *in* Simakov, K.V., and Thurston, D.K., eds., Proceedings of the 1994 International Conference on Arctic Margins: Magadan, Russia, North East Science Center, Far Eastern Branch of the Russian Academy of Science, p. 124–137.

Davis, W.J., 1996, U-Pb geochronology of lower crustal xenoliths from the Archean Slave Province: Evidence for protracted Archean metamorphism and Proterozoic mafic magmatism in the lower crust: Eos (Transactions, American Geophysical Union), v. 77, no. 46, supplement, p. 821.

Dumitru, T.A., Miller, E.L., O'Sullivan, P.B., Amato, J.M., Hannula, K.A., Calvert, A.T., and Gans, P.B., 1995, Cretaceous to recent extension in the Bering Strait region, Alaska: Tectonics, v. 14, p. 549–563.

Gasparik, T., 1984, Experimentally determined stability of clinopyroxene + garnet + corundum in the system CaO-MgO-Al_2O_3-SiO_2: American Mineralogist, v. 69, no. 11–12, p. 1025–1035.

Gibson, G.M., and Ireland, T.R., 1995, Granulite formation during continental extension in Fiordland, New Zealand: Nature, v. 375, p. 479–482.

Green, A.G., Milkereit, B., Percival, J.A., Davidson, A., Parrish, R.R., Cook, F.A., Geis, W.T., Cannon, W.F., Hutchinson, D.R., West, G.F., and Clowes, R.M., 1990, Origin of deep crustal reflections: Seismic profiling across high-grade metamorphic terranes in Canada: Tectonophysics, v. 173, p. 627–638.

Holliger, K., and Levander, A., 1994, Lower crustal reflectivity modelled by rheological controls on mafic intrusions: Geology, v. 22, p. 367–370.

Howell, D.G., Moore, G.W., and Wiley, T.J., 1987, Tectonics and basin evolution of western North America: An overview, *in* Scholl, D.W., Grantz, A., and Vedder, J.G., eds., Geology and resource potential of the continental margin of western North America and adjacent ocean basins: Beaufort Sea to Baja California: Houston, Texas, Circum-Pacific Council for Energy and Mineral Resources, Earth Science Series, v. 6, p. 1–15.

Ivanov, V.V., 1985, Sedimentary basins of North-Eastern Asia (comparative oil and geological analysis): Moscow, Nauka, 208 p. (in Russian).

Law, R.D., Little, T.A., Miller, E.L., and Lee, J., 1994, Extensional origin of ductile fabrics in the Schist Belt, central Brooks Range, Alaska. 2. Quartz fabric studies: Journal of Structural Geology, v. 16, no. 7, p. 919–940.

Little, T.A., Miller, E.L., Lee, J., and Law, R.D., 1994, Extensional origin of ductile fabrics in the Schist Belt, Central Brooks Range, Alaska. 1. Geologic and structural studies: Journal of Structural Geology, v. 16, no. 7, p. 900–918.

Luetgert, J.H., 1992, MacRay: Interactive two-dimensional seismic ray tracing for the Macintosh: U.S. Geological Survey Open-File Report 92–356, 43 p., 1 diskette.

Marlow, M.S, Scholl, D.W., Cooper, A.K., and Buffington, E.C., 1976, Structure and evolution of Bering Sea shelf south of St. Lawrence Island: American Association of Petroleum Geologists Bulletin, v. 60, no. 2, p. 161–183.

Matthews, D.H., and Cheadle, M.J., 1986, Deep reflections from the Caledonides and Variscides west of Britain and comparison with the Himalayas,

in Barazangi, M., and Brown, L.D., eds., Reflection seismology: A global perspective: American Geophysical Union Geodynamics Series, v. 13, p. 5–19.

Matthews, D.H., and the BIRPS Group, 1990, Progress in BIRPS deep seismic reflection profiling around the British Isles: Tectonophysics, v. 173, p. 387–396.

McLean, H., 1977, Organic geochemistry, lithology and paleontology of Tertiary and Mesozoic rocks from wells on the Alaska Peninsula: U.S. Geological Survey Open-File Report N 77–813, 63 p.

McLean, H., 1979, Tertiary stratigraphy and petroleum potential of Cold Bay–False Pass Area, Alaska Peninsula: American Association of Petroleum Geologists Bulletin, v. 63, no. 9, p. 1522–1526.

Miller, E.L., and Hudson, T.L., 1991, Mid-Cretaceous extensional fragmentation of a Jurassic–Early Cretaceous compressional orogen, Alaska: Tectonics, v. 10, p. 781–796.

Miller, E.L., Calvert, A.T., and Little, T.A., 1992, Strain-collapsed metamorphic isograds in a sillimanite gneiss dome, Seward Peninsula, Alaska: Geology, v. 20, p. 487–490.

Miller, T.P., 1994, Pre-Cenozoic plutonic rocks in mainland Alaska, *in* Plafker, G., and Berg, H.C., eds., The geology of Alaska: Boulder, Colorado, Geological Society of America, Geology of North America, v. G-1, p. 589–620.

Moll-Stalcup, E.J., 1994, Latest Cretaceous and Cenozoic magmatism in mainland Alaska, *in* Plafker, G., and Berg, H.C., eds., The geology of Alaska: Boulder, Colorado, Geological Society of America, Geology of North America, v. G-1, p. 589–619.

Mooney, W.D., and Meissner, R., 1992, Multi-genetic origin of crustal reflectivity: A review of seismic reflection profiling of the continental lower crust and Moho, *in* Fountain, D.M., Arculus, R., and Kay, R.W., eds., Continental lower crust: New York, Elsevier, p. 45–71.

Moore, T.E, Wallace, W.K., Bird, K.J., Karl, S.M., Mull, C.G., and Dillon, J.T., 1994, Geology of northern Alaska, *in* Plafker, G., and Berg, H.C., eds., The geology of Alaska: Boulder, Colorado, Geological Society of America, Geology of North America, v. G-1, p. 49–140.

Muir, R.J., Ireland, T.R., Weaver, S.D., and Bradshaw, J.D., 1996a, Ion microprobe dating of Paleozoic granitoids: Devonian magmatism in New Zealand and correlations with Australia and Antarctica: Chemical Geology, v. 127, no. 1–3, p. 191–210.

Muir, R.J., Weaver, S.D., Bradshaw, J.D., Eby, G.N., Evans, J.A., and Ireland, T.R., 1996b, Geochemistry of the Karamea Batholith, New Zealand and comparisons with the Lachlan fold belt granites of SE Australia: Lithos, v. 39, no. 1–2, p. 1–20.

Nelson, K.D., 1992, Are crustal thickness variations in old mountain belts like the Appalachians a consequence of lithospheric delamination?: Geology, v. 20, p. 498–502.

Nokleberg, W.J., Parfenov, L.M., Monger, J.W.H., Baranov, B.V., Byalobzhesky, S.G., Bundtzen, T.K., Fenney, T.D., Fujita, K., Gordey, S.P., Grantz, A., Khanchuk, A.I., Natal'in, B.A., Natapov, L.M., Norton, I.O., Patton, W.W., Jr., Plafker, G., Scholl, D.W., Stone, D.B., Tabor, R.W., Tsukanov, N.V., and Vallier, T.L., 1997, Summary: Circum-Pacific tectonostratigraphic terrane map: U.S. Geological Survey Open-File Report OF 96–0727, scale 1: 10 000 000, 1 sheet.

Nokleberg, W.J., Parfenov, L.M., Monger, J.W.H., Norton, I.O., Khanchuk, A.I., Stone, D.B., Scholl, D.W., and Fujita, K., 1998, Phanerozoic tectonic evolution of the circum-North Pacific: U.S. Geological Survey Open-File Report 98–0754, 125 p.

O'Reilly, S.Y., et al., 1995, Special issue: The xenolith window to the lower crust: Lithos, v. 36, p. 155–306.

Parsons, T., Christiansen, N.I., and Wilshire, H., 1995, Velocities of southern Basin and Range xenoliths: Insights on the nature of lower crustal reflectivity and composition: Geology, v. 23, p. 129–132.

Patton, W.W., and Csejtey, B., 1980, Geologic map of Saint Lawrence Island: U.S. Geological Survey Miscellaneous Investigation Series Map I-203, scale 1:250 000, 1 sheet.

Patton, W.W., Jr., and Dutro, J.T., Jr., 1969, Preliminary report on Paleozoic and Mesozoic sedimentary sequence on Saint Lawrence Island, Alaska, *in* Geological Survey Research 1969: U.S. Geological Survey Professional Paper 650–D, p. D138–D143.

Patton, W.W., Lanphere, M.A., Miller, T.P., and Scott, R.A., 1976, Age and tectonic significance of volcanic rocks in St. Matthew Island, Bering Sea Alaska: U.S. Geological Survey Journal of Research, v. 11, no. 1, p. 67–73.

Rey, P., 1993, Seismic and tectonometamorphic characters of the lower continental crust in Phanerozoic areas, a consequence of post-thickening extension: Tectonics, v. 12, p. 580–590.

Rowe, H., 1998, Petrogenesis of plutons and hypabyssal rocks of the Bering Strait Region, Chukotka, Russia [M.S. thesis]: Houston, Texas, Rice University, 90 p.

Rubin, C.M., Miller, E.L., and Toro, J., 1995, Deformation of the northern circum-Pacific margin: Variations in tectonic style and plate-tectonic implications: Geology, v. 23, p. 897–900.

Rudnick, R.L., 1992, Xenoliths-samples of the lower continental crust, *in* Fountain, D.M., Arculus, R., and Kay, R.W., eds., Continental lower crust: New York, Elsevier, p. 269–308.

Rudnick, R.L., and Fountain, D.M., 1995, Nature and composition of the continental crust: A lower crustal perspective: Reviews of Geophysics, v. 33, p. 267–309.

Rudnick, R.L., and Williams, I.S., 1987, Dating the lower crust by ion microprobe: Earth and Planetary Science Letters, v. 85, p. 145–161.

Till, A.B., and Dumoulin, J.A., 1994, Geology of Seward Peninsula and St. Lawrence Island, *in* Plafker, G., and Berg, H.C., eds., The geology of Alaska: Boulder, Colorado, Geological Society of America, Geology of North America, v. G-1, p. 141–152.

Warner, M.R., 1990, Basalts, water or shear zones in the lower continental crust?: Tectonophysics, v. 173, p. 163–174.

Wilson, F.H., Shew, N., and DuBois, G.D., 1994, Map and table showing isotopic age data in Alaska, *in* Plafker, G., and Berg, H.C., eds., The geology of Alaska: Boulder, Colorado, Geological Society of America, Geology of North America, v. G-1, scale 1:2 500 000, with tables, 1 sheet.

Wirth, K.R., Ronnback, C.M., Grandy, J.S., and Sadofsky, S.J., 1995, Mafic volcanism and xenoliths of the northern Bering Sea Region [abs.]: Eos (Transactions, American Geophysical Union), v. 76, no. 46, supplement, p. 589–590.

Wood, D.A., 1980, The application of a Th-Hf-Ta diagram to problems of tectonomagmatic classifications and to establishing the nature of crustal contamination of basaltic lavas of the British Tertiary volcanic province: Earth and Planetary Science Letters, v. 50, p. 11–30.

Worral, D.M., 1991, Tectonic history of the Bering Sea and the evolution of Tertiary strike-slip basins of the Bering Shelf: Boulder, Colorado, Geological Society of America Special Paper 257, 120 p.

Manuscript Accepted by the Society May 15, 2001.

Printed in the U.S.A.